The American Journal of Human Genetics, Volume *102*

Supplemental Data

Dual Molecular Effects of Dominant *RORA* Mutations Cause Two Variants of Syndromic Intellectual Disability with Either Autism or Cerebellar Ataxia

Claire Guissart, Xenia Latypova, Paul Rollier, Tahir N. Khan, Hannah Stamberger, Kirsty McWalter, Megan T. Cho, Susanne Kjaergaard, Sarah Weckhuysen, Gaetan Lesca, Thomas Besnard, Katrin Õunap, Lynn Schema, Andreas G. Chiocchetti, Marie McDonald, Julitta de Bellescize, Marie Vincent, Hilde Van Esch, Shannon Sattler, Irman Forghani, Isabelle Thiffault, Christine M. Freitag, Deborah Sara Barbouth, Maxime Cadieux-Dion, Rebecca Willaert, Maria J. Guillen Sacoto, Nicole P. Safina, Christèle Dubourg, Lauren Grote, Wilfrid Carré, Carol Saunders, Sander Pajusalu, Emily Farrow, Anne Boland, Danielle Hays Karlowicz, Jean-François Deleuze, Monica H. Wojcik, Rena Pressman, Bertrand Isidor, Annick Vogels, Wim Van Paesschen, Lihadh Al-Gazali, Aisha Mohamed Al Shamsi, Mireille Claustres, Aurora Pujol, Stephan J. Sanders, François Rivier, Nicolas Leboucq, Benjamin Cogné, Souphatta Sasorith, Damien Sanlaville, Kyle Retterer, Sylvie Odent, Nicholas Katsanis, Stéphane Bézieau, Michel Koenig, Erica E. Davis, Laurent Pasquier, and Sébastien Küry

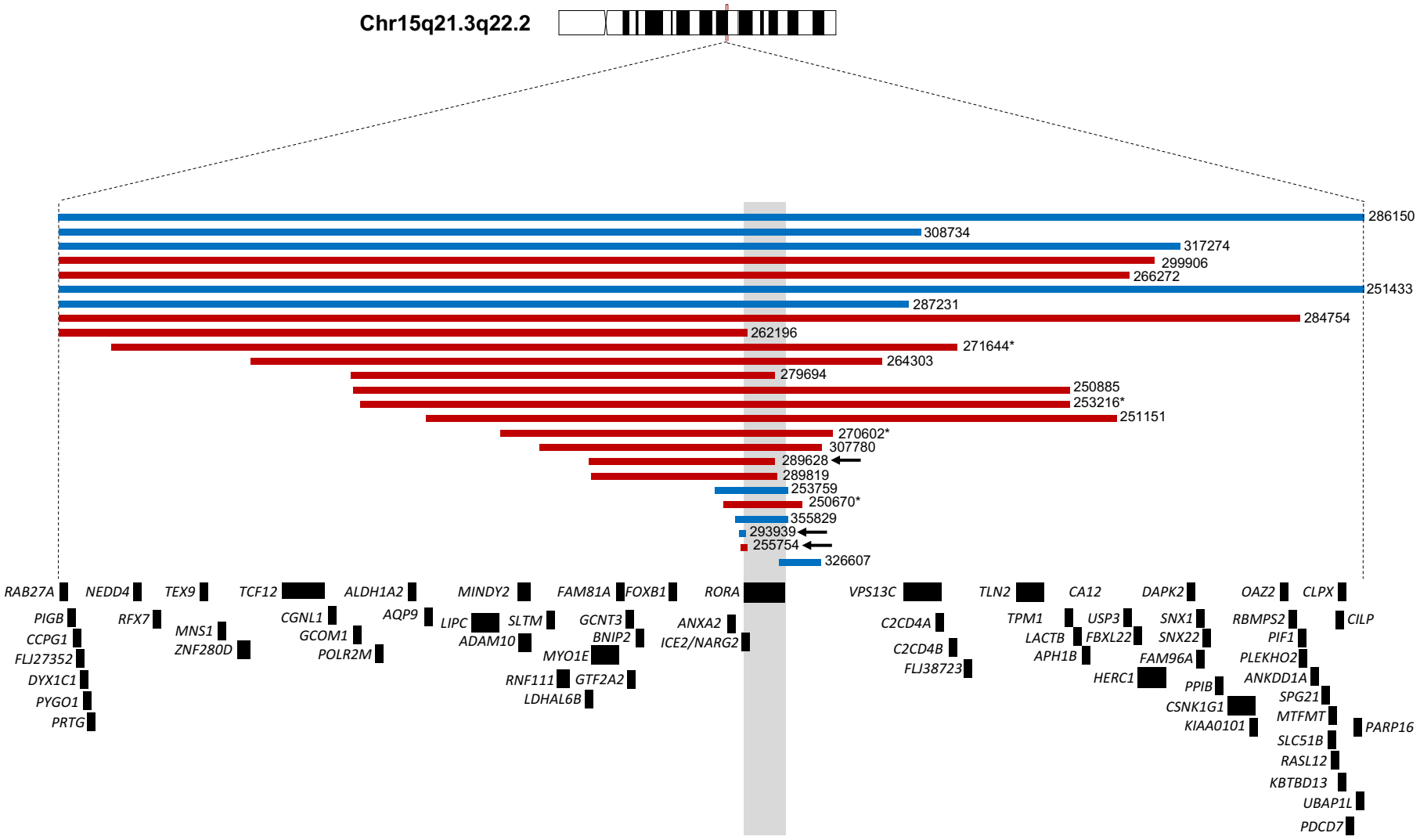
Chr15q21.3q22.2
286150
308734
317274
299906
266272
251433
287231
284754
262196
271644*
264303
279694
250885
253216*
251151
270602*
307780
289628
289819
253759
250670*
355829
293939
255754
326607
RAB27A
NEDD4
TEX9
TCF12
ALDH1A2
MINDY2
FAM81A
FOXB1
RORA
VPS13C
TLN2
CA12
DAPK2
OAZ2
CLPX
PIGB
RFX7
CGNL1
AQP9
LIPC
SLTM
GCNT3
ANXA2
C2CD4A
TPM1
USP3
SNX1
RBMPS2
CILP
CCPG1
MNS1
GCOM1
ADAM10
BNIP2
ICE2/NARG2
C2CD4B
LACTB
FBXL22
SNX22
PIF1
FLJ27352
ZNF280D
POLR2M
MYO1E
FLJ38723
APH1B
FAM96A
PLEKHO2
DYX1C1
RNF111
GTF2A2
HERC1
ANKDD1A
PYGO1
LDHAL6B
PPIB
SPG21
PRTG
CSNK1G1
MTFMT
PARP16
KIAA0101
SLC51B
RASL12
KBTBD13
UBAP1L
PDCD7

Figure S1

Figure S1. Schematic of copy number variants in the DECIPHER database encompassing the *RORA* locus on 15q22. Copy number loss (deletion) is shown in red; copy number gain (duplication) is shown in blue. DECIPHER individual case numbers are provided. Individuals included in our study are marked by arrows, and individuals reported previously (Yamamoto et al., 2014) are indicated by asterisks. Vertical gray shaded bar indicates the *RORA* locus. Database query was conducted in December 2017.

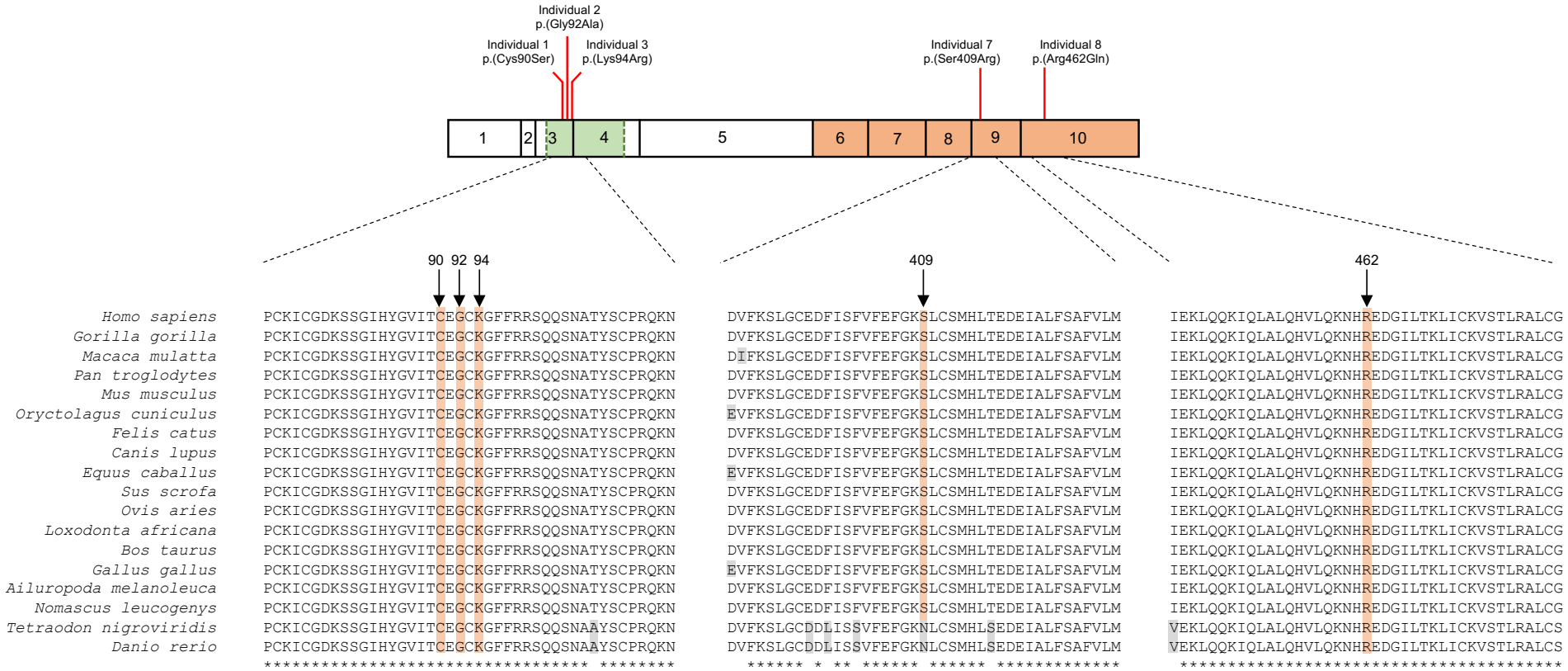
Individual 2
p.(Gly92Ala)
Individual 1
p.(Cys90Ser)
Individual 3
p.(Lys94Arg)
Individual 7
p.(Ser409Arg)
Individual 8
p.(Arg462Gln)
1
2
3
4
5
6
7
8
9
10
90 92 94
409
462
Homo sapiens PCKICGDKSSGIHYGVITCEGCKGFFRRSQQSNATYSCPRQKN DVFKSLGCEDFISFVFEFGKSLCSMHLTEDEIALFSAFVLM IEKLQQKIQLALQHVLQKNHREDGILTKLICKVSTLRALCG
Gorilla gorilla PCKICGDKSSGIHYGVITCEGCKGFFRRSQQSNATYSCPRQKN DVFKSLGCEDFISFVFEFGKSLCSMHLTEDEIALFSAFVLM IEKLQQKIQLALQHVLQKNHREDGILTKLICKVSTLRALCG
Macaca mulatta PCKICGDKSSGIHYGVITCEGCKGFFRRSQQSNATYSCPRQKN DIFKSLGCEDFISFVFEFGKSLCSMHLTEDEIALFSAFVLM IEKLQQKIQLALQHVLQKNHREDGILTKLICKVSTLRALCG
Pan troglodytes PCKICGDKSSGIHYGVITCEGCKGFFRRSQQSNATYSCPRQKN DVFKSLGCEDFISFVFEFGKSLCSMHLTEDEIALFSAFVLM IEKLQQKIQLALQHVLQKNHREDGILTKLICKVSTLRALCG
Mus musculus PCKICGDKSSGIHYGVITCEGCKGFFRRSQQSNATYSCPRQKN DVFKSLGCEDFISFVFEFGKSLCSMHLTEDEIALFSAFVLM IEKLQQKIQLALQHVLQKNHREDGILTKLICKVSTLRALCG
Oryctolagus cuniculus PCKICGDKSSGIHYGVITCEGCKGFFRRSQQSNATYSCPRQKN EVFKSLGCEDFISFVFEFGKSLCSMHLTEDEIALFSAFVLM IEKLQQKIQLALQHVLQKNHREDGILTKLICKVSTLRALCG
Felis catus PCKICGDKSSGIHYGVITCEGCKGFFRRSQQSNATYSCPRQKN DVFKSLGCEDFISFVFEFGKSLCSMHLTEDEIALFSAFVLM IEKLQQKIQLALQHVLQKNHREDGILTKLICKVSTLRALCG
Canis lupus PCKICGDKSSGIHYGVITCEGCKGFFRRSQQSNATYSCPRQKN DVFKSLGCEDFISFVFEFGKSLCSMHLTEDEIALFSAFVLM IEKLQQKIQLALQHVLQKNHREDGILTKLICKVSTLRALCG
Equus caballus PCKICGDKSSGIHYGVITCEGCKGFFRRSQQSNATYSCPRQKN EVFKSLGCEDFISFVFEFGKSLCSMHLTEDEIALFSAFVLM IEKLQQKIQLALQHVLQKNHREDGILTKLICKVSTLRALCG
Sus scrofa PCKICGDKSSGIHYGVITCEGCKGFFRRSQQSNATYSCPRQKN DVFKSLGCEDFISFVFEFGKSLCSMHLTEDEIALFSAFVLM IEKLQQKIQLALQHVLQKNHREDGILTKLICKVSTLRALCG
Ovis aries PCKICGDKSSGIHYGVITCEGCKGFFRRSQQSNATYSCPRQKN DVFKSLGCEDFISFVFEFGKSLCSMHLTEDEIALFSAFVLM IEKLQQKIQLALQHVLQKNHREDGILTKLICKVSTLRALCG
Loxodonta africana PCKICGDKSSGIHYGVITCEGCKGFFRRSQQSNATYSCPRQKN DVFKSLGCEDFISFVFEFGKSLCSMHLTEDEIALFSAFVLM IEKLQQKIQLALQHVLQKNHREDGILTKLICKVSTLRALCG
Bos taurus PCKICGDKSSGIHYGVITCEGCKGFFRRSQQSNATYSCPRQKN DVFKSLGCEDFISFVFEFGKSLCSMHLTEDEIALFSAFVLM IEKLQQKIQLALQHVLQKNHREDGILTKLICKVSTLRALCG
Gallus gallus PCKICGDKSSGIHYGVITCEGCKGFFRRSQQSNATYSCPRQKN EVFKSLGCEDFISFVFEFGKSLCSMHLTEDEIALFSAFVLM IEKLQQKIQLALQHVLQKNHREDGILTKLICKVSTLRALCG
Ailuropoda melanoleuca PCKICGDKSSGIHYGVITCEGCKGFFRRSQQSNATYSCPRQKN DVFKSLGCEDFISFVFEFGKSLCSMHLTEDEIALFSAFVLM IEKLQQKIQLALQHVLQKNHREDGILTKLICKVSTLRALCG
Nomascus leucogenys PCKICGDKSSGIHYGVITCEGCKGFFRRSQQSNATYSCPRQKN DVFKSLGCEDFISFVFEFGKSLCSMHLTEDEIALFSAFVLM IEKLQQKIQLALQHVLQKNHREDGILTKLICKVSTLRALCG
Tetraodon nigroviridis PCKICGDKSSGIHYGVITCEGCKGFFRRSQQSNAAYSCPRQKN DVFKSLGCDDLISSVFEFGKNLCSMHLSEDEIALFSAFVLM VEKLQQKIQLALQHVLQKNHREDGILTKLICKVSTLRALCS
Danio rerio PCKICGDKSSGIHYGVITCEGCKGFFRRSQQSNAAYSCPRQKN DVFKSLGCDDLISSVFEFGKNLCSMHLSEDEIALFSAFVLM VEKLQQKIQLALQHVLQKNHREDGILTKLICKVSTLRALCS

Figure S2

Figure S2. Multiple protein sequence alignment of RORA orthologs across vertebrate species show conservation of missense mutations detected in cases. Schematic of the RORa protein (NP_599023.1) and its domains (DNA binding domain, green; ligand binding domain, orange) and location of each of the missense variants reported in this study (top). Protein sequence alignments from 18 vertebrate species is shown (bottom). Orange shading in the alignment indicates RORA amino acids Cys90, Gly92, Lys94, Ser409, and Arg462. Grey shading indicates species-specific non-conserved amino acids. Asterisk indicates 100% conservation across mentioned species. Multiple sequence alignment was performed with ClustalW using the following UniProt identifiers: P35398, *Homo sapiens*; G3QE47, *Gorilla gorilla*; F7E9K9, *Macaca mulatta*; H2R8C9, *Pan troglodytes*; P51448, *Mus musculus*; G1T4B2, *Oryctolagus cuniculus*; M3WJ80, *Felis catus*; F1P607, *Canis lupus*; F6X794, *Equus caballus*; F1S075, *Sus scrofa*; W5QI24, *Ovis aries*; G3SLZ5, *Loxodonta africana*; F1N7R0, *Bos taurus*; F1NML9, *Gallus gallus*; G1LN19, *Ailuropoda melanoleuca*; G1RMH6, *Nomascus leucogenys*; H3CSJ1, *Tetraodon nigroviridis*; A7VL70, *Danio rerio*.

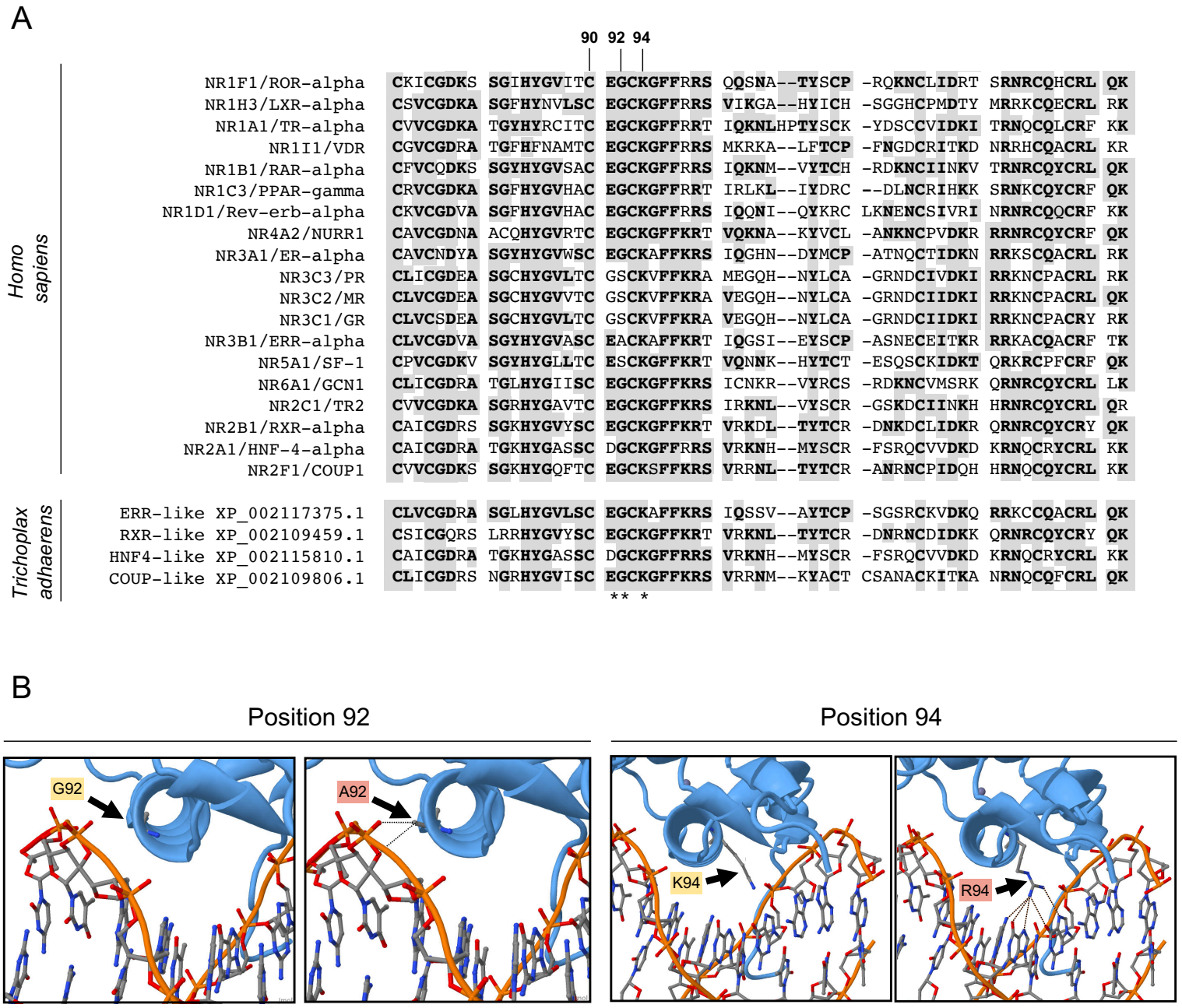
A
90 92 94
Homo sapiens
NR1F1/ROR-alpha CKICGDKS SGIHYGVITC EGCKGFFRRS QQSNA--TYSCP -RQKNCLIDRT SRNRCQHCRL QK
NR1H3/LXR-alpha CSVCGDKA SGFHYNVLSC EGCKGFFRRS VIKGA--HYICH -SGGHCPMDTY MRRKCQECRL RK
NR1A1/TR-alpha CVVCGDKA TGYHYRCITC EGCKGFFRRT IQKNLHPTYSCK -YDSCCVIDKI TRNQCQLCRF KK
NR1I1/VDR CGVCGDRA TGFHFNAMTC EGCKGFFRRS MKRKA--LFTCP -FNGDCRITKD NRRHCQACRL KR
NR1B1/RAR-alpha CFVCQDKS SGYHYGVSAC EGCKGFFRRS IQKNM--VYTCH -RDKNCIINKV TRNRCQYCRL QK
NR1C3/PPAR-gamma CRVCGDKA SGFHYGVHAC EGCKGFFRRT IRLKL--IYDRC --DLNCRIHKK SRNKCQYCRF QK
NR1D1/Rev-erb-alpha CKVCGDVA SGFHYGVHAC EGCKGFFRRS IQQNI--QYKRC LKNENCSIVRI NRNRCQQCRF KK
NR4A2/NURR1 CAVCGDNA ACQHYGVRTC EGCKGFFKRT VQKNA--KYVCL -ANKNCPVDKR RRNRCQYCRF QK
NR3A1/ER-alpha CAVCNDYA SGYHYGVWSC EGCKAFFKRS IQGHN--DYMCP -ATNQCTIDKN RRKSCQACRL RK
NR3C3/PR CLICGDEA SGCHYGVLTC GSCKVFFKRA MEGQH--NYLCA -GRNDCIVDKI RRKNCPACRL RK
NR3C2/MR CLVCGDEA SGCHYGVVTC GSCKVFFKRA VEGQH--NYLCA -GRNDCIIDKI RRKNCPACRL QK
NR3C1/GR CLVCSDEA SGCHYGVLTC GSCKVFFKRA VEGQH--NYLCA -GRNDCIIDKI RRKNCPACRY RK
NR3B1/ERR-alpha CLVCGDVA SGYHYGVASC EACKAFFKRT IQGSI--EYSCP -ASNECEITKR RRKACQACRF TK
NR5A1/SF-1 CPVCGDKV SGYHYGLLTC ESCKGFFKRT VQNNK--HYTCT -ESQSCKIDKT QRKRCPFCRF QK
NR6A1/GCN1 CLICGDRA TGLHYGIISC EGCKGFFKRS ICNKR--VYRCS -RDKNCVMSRK QRNRCQYCRL LK
NR2C1/TR2 CVVCGDKA SGRHYGAVTC EGCKGFFKRS IRKNL--VYSCR -GSKDCIINKH HRNRCQYCRL QR
NR2B1/RXR-alpha CAICGDRS SGKHYGVYSC EGCKGFFKRT VRKDL--TYTCR -DNKDCLIDKR QRNRCQYCRY QK
NR2A1/HNF-4-alpha CAICGDRA TGKHYGASSC DGCKGFFRRS VRKNH--MYSCR -FSRQCVVDKD KRNQCRYCRL KK
NR2F1/COUP1 CVVCGDKS SGKHYGQFTC EGCKSFFKRS VRRNL--TYTCR -ANRNCPIDQH HRNQCQYCRL KK
Trichoplax adhaerens
ERR-like XP_002117375.1 CLVCGDRA SGLHYGVLSC EGCKAFFKRS IQSSV--AYTCP -SGSRCKVDKQ RRKCCQACRL QK
RXR-like XP_002109459.1 CSICGQRS LRRHYGVYSC EGCKGFFKRT VRKNL--TYTCR -DNRNCDIDKK QRNRCQYCRY QK
HNF4-like XP_002115810.1 CAICGDRA TGKHYGASSC DGCKGFFRRS VRKNH--MYSCR -FSRQCVVDKD KRNQCRYCRL KK
COUP-like XP_002109806.1 CLICGDRS NGRHYGVISC EGCKGFFKRS VRRNM--KYACT CSANACKITKA NRNQCQFCRL QK
** *
B
Position 92
Position 94
G92
A92
K94
R94

Figure S3

Figure S3. 3D modeling and sequence conservation of the first zinc finger motif of the RORa DNA-binding domain. (**A**) Sequence comparison of amino acids in the conserved DNA binding domain of human paralogous nuclear receptor proteins and of the four *Trichoplax adhaerens* (primitive metazoan) orthologs. The identifier following "NR" indicates the sub-family to which the nuclear receptors belong. Amino acids that match the consensus sequence are shown in bold and shaded gray. Residue numbering at the top of the alignment corresponds to RORa isoform a. The mutated amino acid cysteine (C) 90, glycine (G) 92, and lysine (K) 94 are indicated on top. Amino acids involved in the P-box are indicated by an asterisk (*). (**B**) Homology model of RORa DNA-binding domain in complex with RORE (ROR DNA response element consisting of the consensus core motif AGGTCA). RORa is depicted in blue as a backbone carbon CA trace and atoms are represented in a standard color scheme. Modeled interaction of RORa isoform a (NP_599023.1) wild type (WT) Gly92 and variant Ala92 (left) or WT Lys94 and variant Arg94 (right) in the recognition a-helix of the RORa DBD with the major groove of DNA. For either mutant, the putative clash between RORa DBD and the DNA are represented by black dotted lines. Clashes between the RORa DBD indicate either distances too short for van der Waals interaction (Ala92-phosphate backbone; left), or for hydrogen bonds (Lys94-guanine-guanine and complementary cytosine; right).

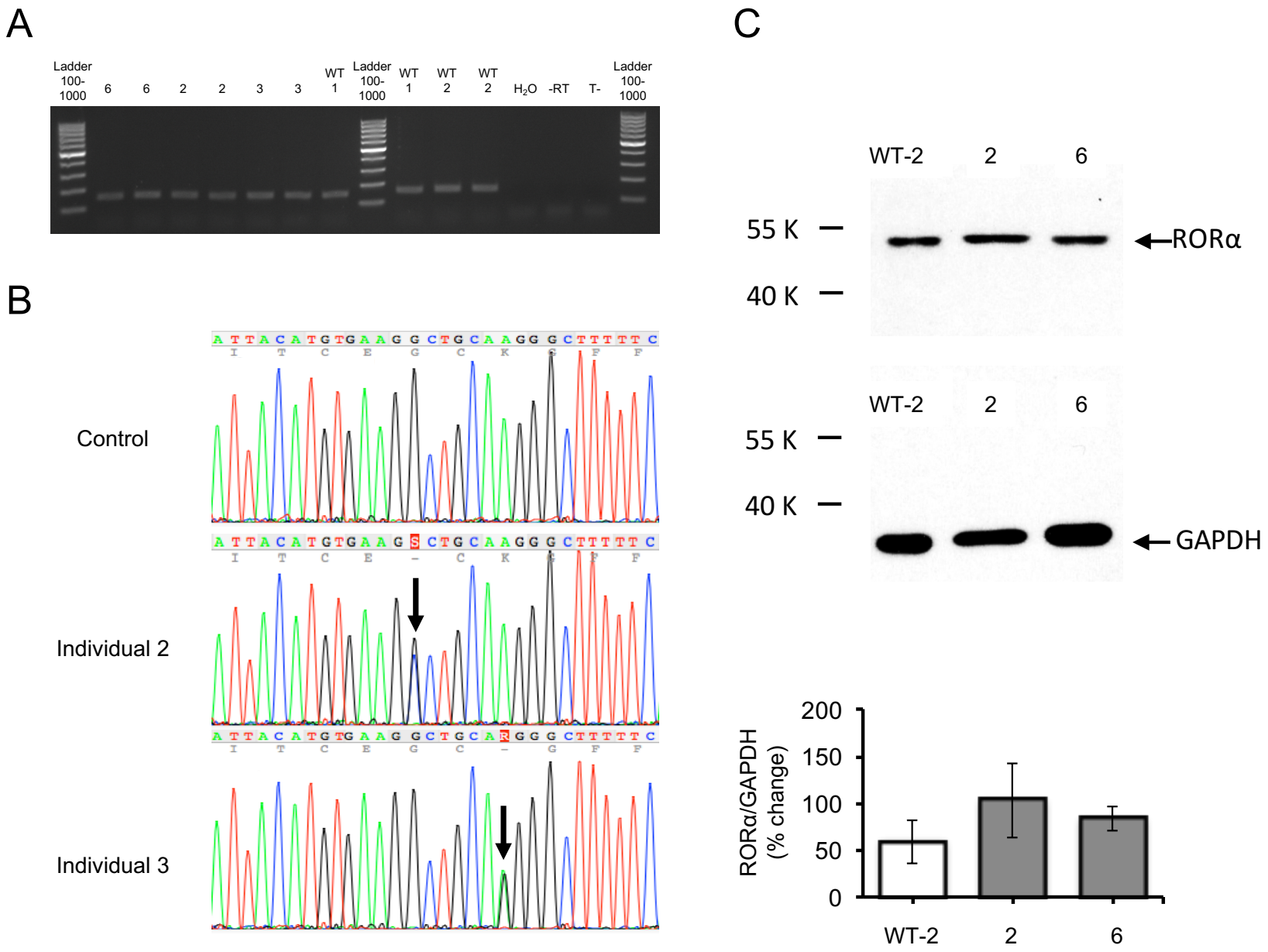
A
Ladder 100-1000
6
6
2
2
3
3
WT 1
Ladder 100-1000
WT 1
WT 2
WT 2
H2O
-RT
T-
Ladder 100-1000
B
Control
Individual 2
Individual 3
C
WT-2
2
6
55 K
40 K
RORα
WT-2
2
6
55 K
40 K
GAPDH
RORα/GAPDH (% change)
200
150
100
50
0
WT-2
2
6

Figure S4

Figure S4. Molecular and biochemical characterization of RORA variants. (**A**) RT-PCR analysis of a 152bp fragment of *RORA* cDNA encompassing the c.281A>G mutation in affected individuals 2, 3 and 6 and control individuals (WT1 and WT2). c.282G is the last nucleotide of exon 3 of *RORA* (NM_134261.2). Neither abnormal sized product nor semi-quantitative variation was observed, suggesting unimpaired splicing. (**B**) Sequencing of the *RORA* RT-PCR products, showing the presence of missense changes c.275G>C (p.Gly92Ala) and c.281A>G (p.Lys94Arg) in individuals 2 and 3, respectively. (**C**) Western blot analysis of protein lysates derived skin fibroblasts established from individual 2 and 6, and control individual WT2. The anti-RORα antibodies were probed against fibroblast cell lysate and revealed a band of the expected size (55 kDa). No smaller product was detected, in particular no truncated fragment was detected for individual 6 bearing a heterozygous frame-shift mutation. The blot was reprobed with anti-GAPDH antibodies. The results show a moderate increase of RORα levels in individual 2 and 6 when compared with wild-type levels as indicated by densitometry analysis. Quantification is based on 3 measurements (individuals 2 and 6) or 4 measurements (WT-2). A representative result of the Western blots is shown. Error bars represent standard error of the mean.

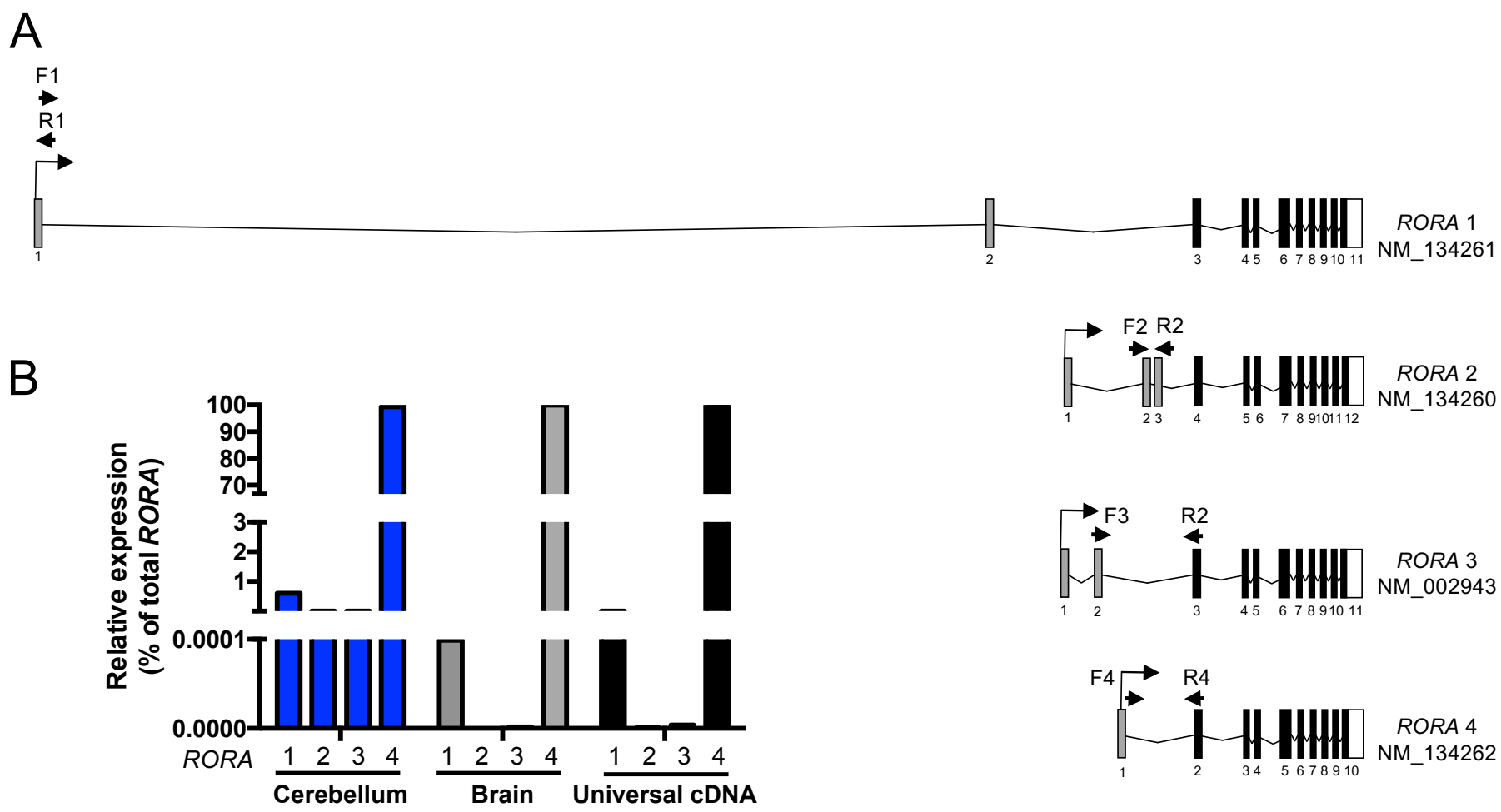
A
F1
R1
1
2
3
4 5
6 7 8 9 10 11
RORA 1
NM_134261
F2 R2
1
2 3
4
5 6
7 8 9 10 11 12
RORA 2
NM_134260
F3
R2
1
2
3
4 5
6 7 8 9 10 11
RORA 3
NM_002943
F4
R4
1
2
3 4
5 6 7 8 9 10
RORA 4
NM_134262
B
Relative expression
(% of total RORA)
100
90
80
70
3
2
1
0.0001
0.0000
RORA
1 2 3 4
1 2 3 4
1 2 3 4
Cerebellum
Brain
Universal cDNA

Figure S5

Figure S5. *RORA* encodes four protein coding splice variants. (**A**) Schematic of the four splice variants expressed from the human *RORA* locus with RefSeq annotations. Gray boxes, coding exons that are unique to each transcript; black boxes, coding exons that are shared among the four transcripts; white boxes, untranslated regions. Arrows indicate position of oligonucleotides used for qRT-PCR experiments. (**B**) *RORA* 4 is the major splice isoform expressed in the central nervous system. qRT-PCR was performed on control adult human cDNA and analyzed by the ΔCt method with normalization to ß-actin mRNA expression. Canonical isoform *RORA* 1 is weakly expressed, as well as *RORA* 2 and *RORA* 3.

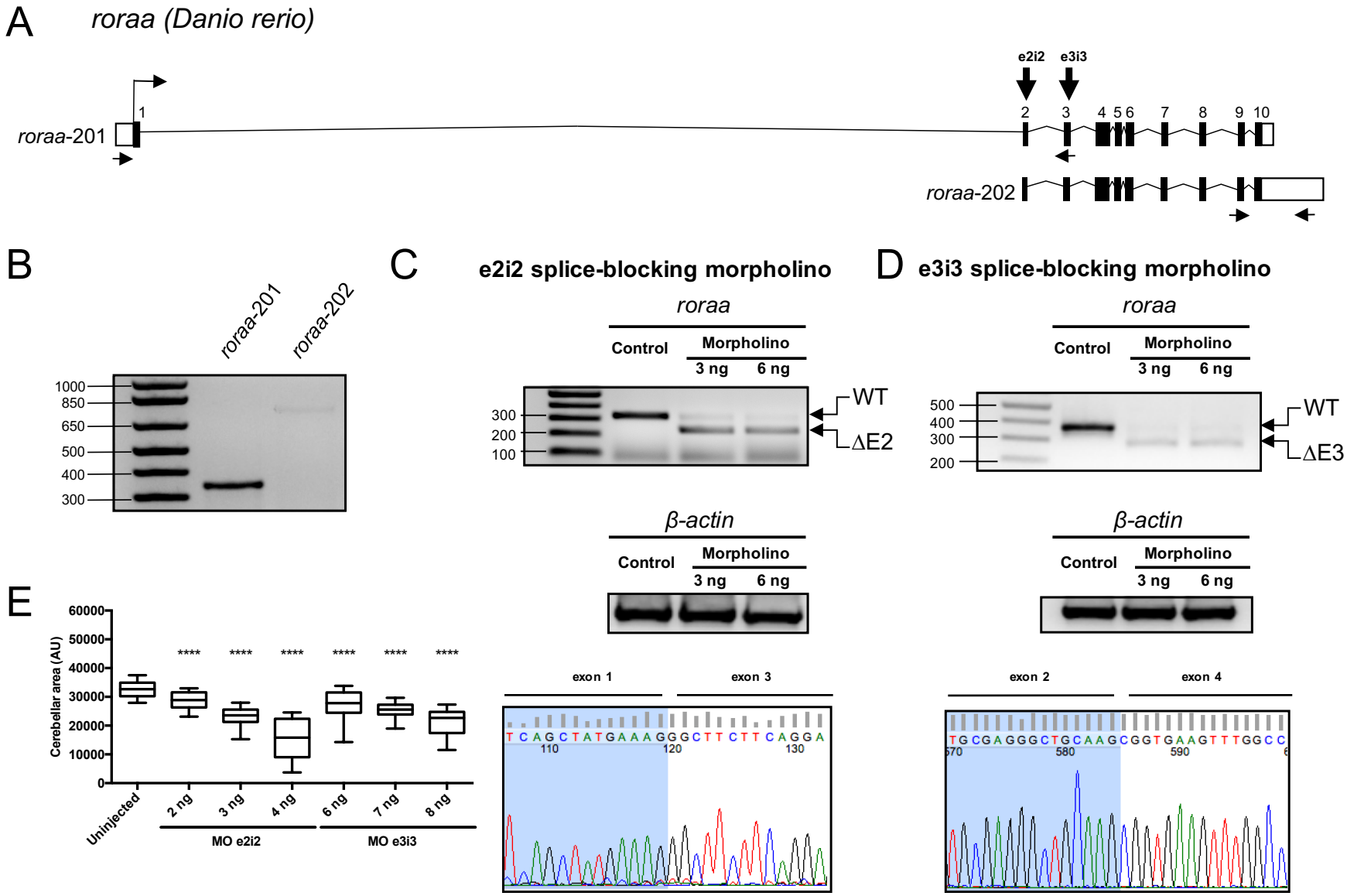
A
roraa (Danio rerio)
roraa-201
roraa-202
e2i2
e3i3
1
2
3
4 5 6
7
8
9 10
B
roraa-201
roraa-202
1000
850
650
500
400
300
C
e2i2 splice-blocking morpholino
roraa
Control
Morpholino
3 ng
6 ng
300
200
100
WT
ΔE2
β-actin
exon 1
exon 3
T C A G C T A T G A A A G G G C T T C T T C A G G A
110
120
130
D
e3i3 splice-blocking morpholino
roraa
Control
Morpholino
3 ng
6 ng
500
400
300
200
WT
ΔE3
β-actin
exon 2
exon 4
T G C G A G G G C T G C A A G C G G T G A A G T T T G G C C
570
580
590
E
Cerebellar area (AU)
60000
50000
40000
30000
20000
10000
0
****
Uninjected
2 ng
3 ng
4 ng
6 ng
7 ng
8 ng
MO e2i2
MO e3i3

Figure S6

Figure S6. *roraa* morpholino targeting efficiency. (**A**) Schematic of two zebrafish *roraa* transcripts, *roraa*-201 and *roraa*-202 (genome assembly Zv10); coding regions, black boxes; untranslated regions, white boxes. Zebrafish *roraa*-201 encodes GenBank ID: NP_001103637 (95% similar; 91% identical to human RORA 4). Vertical arrows indicate splice-blocking (sb) morpholino (MO) target sites on the donor sites of exons 2 and 3, respectively; horizontal arrows indicate RT-PCR primers used to generate amplicons in panel **B**. (**B**) *roraa*-201 and *rora*-202 are detectable in zebrafish during larval development (3 days post-fertilization, dpf). Agarose gel image showing RT-PCR results obtained by using isoform-specific primers (shown in panel **A**). (**C**) Agarose gel images (top), and chromatograms of TOPO-cloned PCR product (bottom) demonstrate that the e2i2 sb MO induces exclusion of exon 2 (DE2) leading to a frameshift and introduction of a premature stop codon (p.Ile62*); WT, wild-type transcript. (**D**) Agarose gel images (top), and chromatogram of TOPO-cloned PCR product (bottom) shows that the e3i3 sb MO leads to skipping of exon 3 (DE3) leading to a frameshift and premature stop codon (p.Val88*). (**E**) *roraa* e2i2 or e3i3 sb MOs lead to dose-dependent reduction of cerebellar size in 3 dpf larval batches immunostained with anti-acetylated tubulin antibody. Stars indicate *P* value compared to WT; ****, $p<0.0001$. Error bars in (**E**) re-present 5th and 95th Percentile.

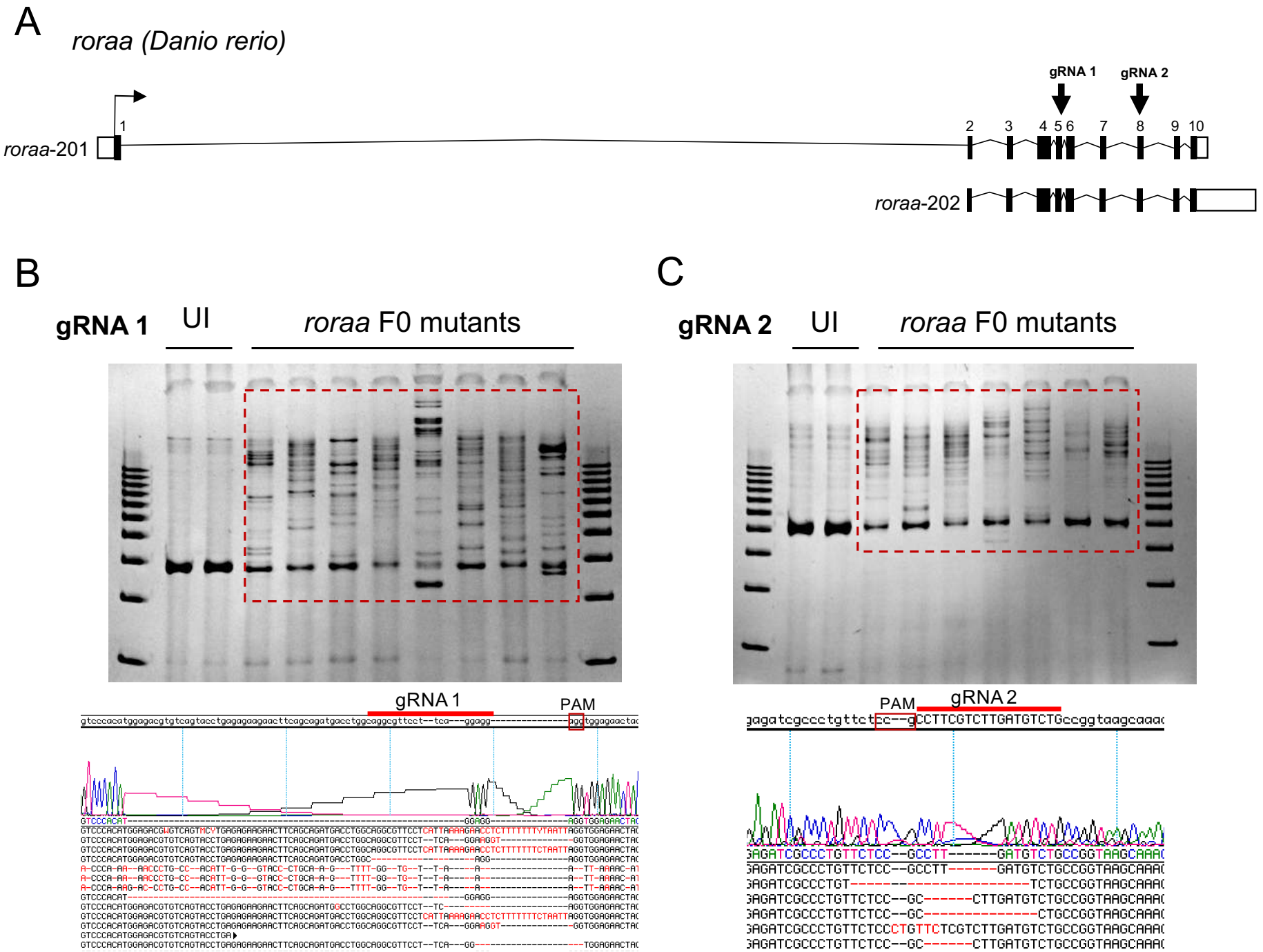
A
roraa (Danio rerio)
gRNA 1
gRNA 2
roraa-201
1
2 3 4 5 6 7 8 9 10
roraa-202
B
gRNA 1
UI
roraa F0 mutants
gRNA 1
PAM
C
gRNA 2
UI
roraa F0 mutants
PAM
gRNA 2

Figure S7

Figure S7. *roraa* CRISPR/Cas9 genome editing efficiency. (**A**) Schematic of two zebrafish *roraa* transcripts, *roraa*-201 and *roraa*-202 (genome assembly Zv10); coding regions, black boxes; untranslated regions, white boxes. guide (g)RNA target sites are by vertical arrows on exons 5 and 8. (**B** and **C**) Top, CRISPR/Cas9 targeting of *roraa* F0 mutant embryos leads to small insertion and deletion events detectable by heteroduplex formation; PCR products flanking target sites were amplified, denatured, slowly reannealed and migrated on a polyacrylamide gel (n=2 uninjected [UI] controls and 8 or 7 F0 mutants for gRNA 1 and gRNA 2, respectively). Heteroduplexes are indicated by red boxes. Bottom, representative chromatograms indicating insertion and deletion events at the gRNA target. gRNA sequence and protospacer adjacent motifs (PAM) are shown. We sequenced 3 F0 mutants/gRNA and 24 colonies per embryo to confirm >90% mosaicism for both gRNA 1 and gRNA 2.

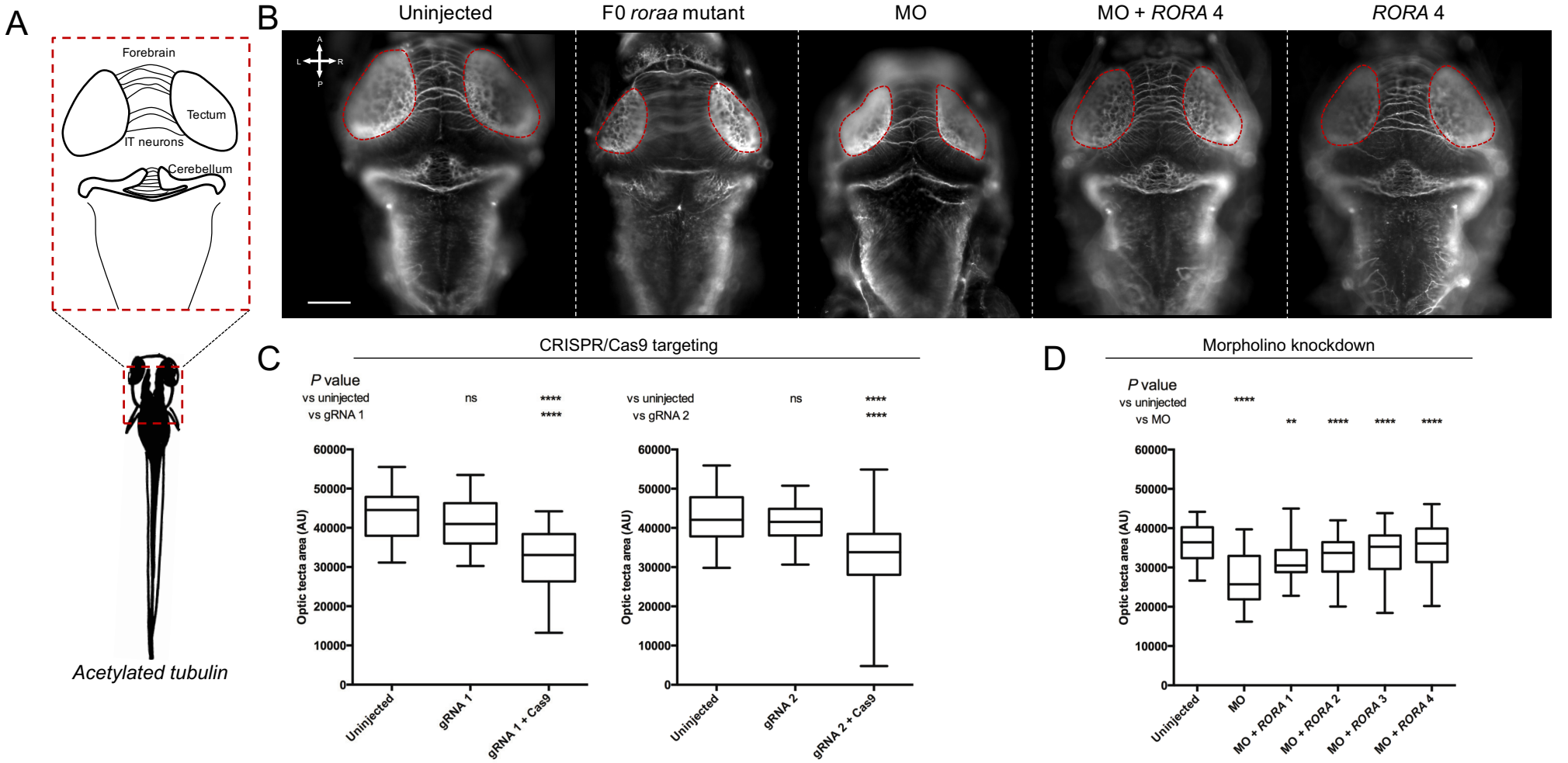
A
Forebrain
Tectum
IT neurons
Cerebellum
Acetylated tubulin
B
Uninjected
F0 roraa mutant
MO
MO + RORA 4
RORA 4
C
CRISPR/Cas9 targeting
P value
vs uninjected
vs gRNA 1
ns
****
****
vs uninjected
vs gRNA 2
ns
****
****
Optic tecta area (AU)
60000
50000
40000
30000
20000
10000
0
Uninjected
gRNA 1
gRNA 1 + Cas9
Uninjected
gRNA 2
gRNA 2 + Cas9
D
Morpholino knockdown
P value
vs uninjected
vs MO
****
**
****
****
****
Optic tecta area (AU)
Uninjected
MO
MO + RORA 1
MO + RORA 2
MO + RORA 3
MO + RORA 4

Figure S8

Figure S8. Disruption of *roraa* in zebrafish larvae results in a reduction of optic tecta size. (**A**) Schematic of neuroanatomical structures painted with anti-acetylated tubulin antibody at 3 days post fertilization (dpf); IT, intertectal. (**B**) Representative dorsal images of acetylated tubulin immunostained larvae show that *roraa* ablation causes neuroanatomical defects in CRISPR/Cas9 F0 mutants and morphants. Optic tecta size was measured as indicated by the dashed red outline on inset panels. Scale bar: 100 μm. (**C**) Quantification of tecta area in larval batches is shown for two guide (g)RNAs targeting either *roraa* exon 5 (gRNA 1) or exon 8 (gRNA 2) (**D**) *roraa* morphants (injected with 3 ng morpholino; MO) display a neuroanatomical phenotype that can be rescued by four different wild type *RORA* mRNA transcripts: co-injection of *roraa* e2i2 splice-blocking MO with *RORA* splice variants (*RORA* 1: NM_134261, *RORA* 2: NM_134260, *RORA* 3: NM_002943 and *RORA* 4: NM_134262). AU, arbitrary units. Stars indicate *P* value compared to uninjected controls (CRISPR/Cas9 and MO) or to morphants (MO + RORA). ****, $p<0.0001$; **, $p<0.01$; ns, not significant. Error bars in (**C**) and (**D**) represent 5th and 95th Percentile.

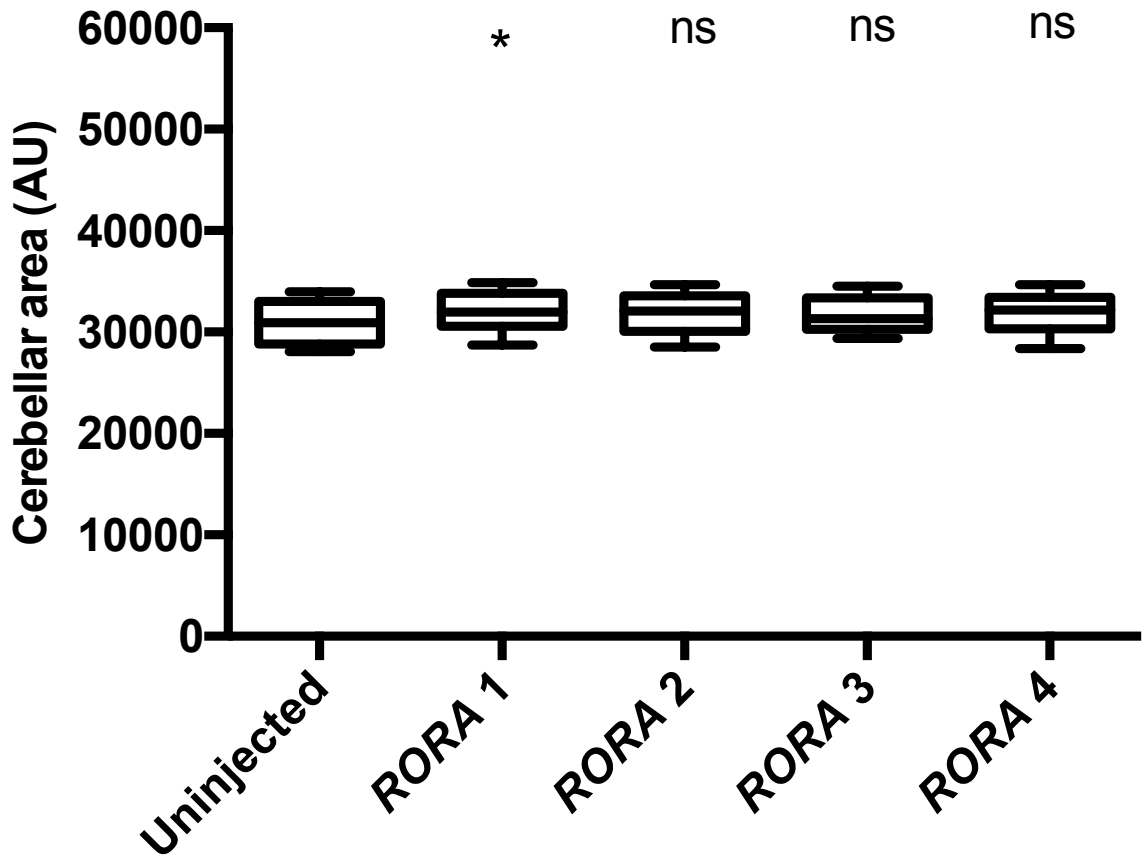
60000
50000
40000
30000
20000
10000
0
Cerebellar area (AU)
*
ns
ns
ns
Uninjected
RORA 1
RORA 2
RORA 3
RORA 4

Figure S9

Figure S9. Ectopic expression of human WT *RORA* in zebrafish larvae. *In vivo* ectopic expression of *RORA* splice variants does not induce cerebellar abnormalities. Zebrafish embryos were injected with 200 pg of wild-type *RORA* mRNA corresponding to each of the four protein coding isoforms, stained with acetylated tubulin antibody, imaged and measured (see Figure 3). AU, arbitrary units. *P* values are not significant (ns) except for *RORA* 1: $P=0.03$ (bilateral t-test). Error bars represent 5th and 95th Percentile.

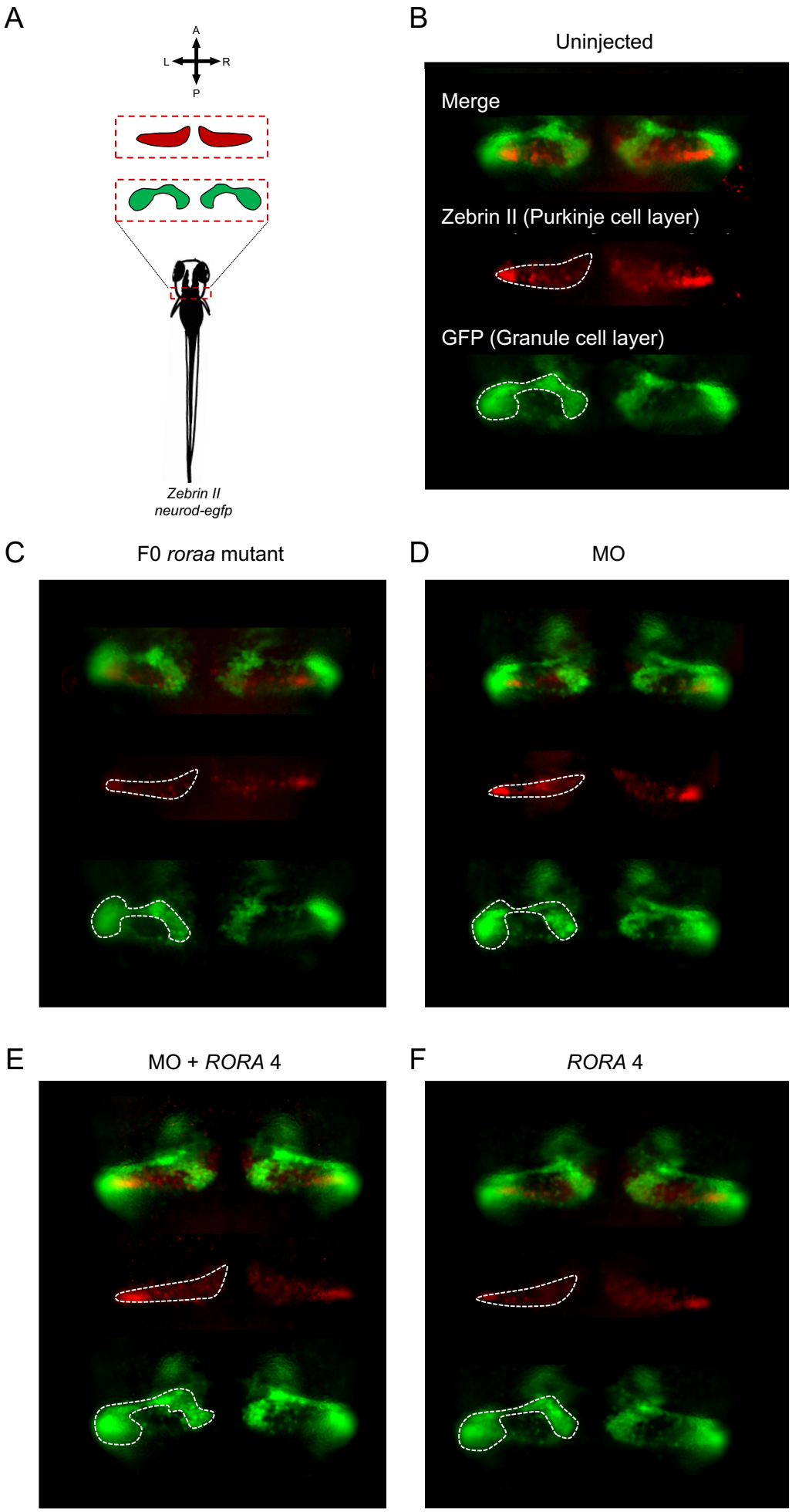
A
A
L
R
P
Zebrin II
neurod-egfp
B
Uninjected
Merge
Zebrin II (Purkinje cell layer)
GFP (Granule cell layer)
C
F0 roraa mutant
D
MO
E
MO + RORA 4
F
RORA 4

Figure S10

Figure S10. Disruption of *roraa* in zebrafish larvae results in cerebellar hypoplasia driven by Purkinje and granule cell loss. (**A**) Schematic of cerebellar cell types assessed in 3 dpf larvae using either a *neurod:egfp* transgene (green) or anti-zebrin II immunostaining (red). Orientation is indicated with A, anterior; P, posterior; L, left; R, right. (**B-F**) Representative dorsal images show that reduction of Purkinje and granule cells contributes to cerebellar defects induced by *roraa* targeting. Transgenic *neurod:egfp* larvae were fixed, immunostained with anti-zebrin II antibody (red), and the area comprised of each cell type was measured (as indicated in the schematic; see Figure 3E-H). Dashed white lines indicate measured area in (**B**) uninjected larvae; (**C**) larvae injected with CRISPR/Cas9 cocktail; (**D**) e2i2 splice-blocking morpholino (MO); (**E**) MO co-injected with wild-type *RORA* 4 mRNA; or (**F**) wild-type *RORA* mRNA alone.